Published in final edited form as:
Cell Signal. 2012 June ; 24(6): 1126–1133. doi:10.1016/j.cellsig.2011.12.020.

Ceramide Kinase Regulates TNFα-Stimulated NADPH Oxidase Activity and Eicosanoid Biosynthesis in Neuroblastoma Cells

Brian M. Barth[a,b], **Sally J. Gustafson**[a,c], **Jody L. Hankins**[b], **James M. Kaiser**[b], **Jeremy K. Haakenson**[b], **Mark Kester**[b], and **Thomas B. Kuhn**[a]

Brian M. Barth: bmb14@psu.edu; Sally J. Gustafson: sjbrown@alaska.edu; Jody L. Hankins: jlh59@psu.edu; James M. Kaiser: jmk39@psu.edu; Jeremy K. Haakenson: jkh190@psu.edu; Mark Kester: mxk38@psu.edu

[a]Department of Chemistry and Biochemistry, University of Alaska-Fairbanks, 900 Yukon Drive, Fairbanks, AK 99775

[b]Department of Pharmacology, College of Medicine, Pennsylvania State University, 500 University Drive, PO Box 850, Hershey, PA 17033

Abstract

A persistent inflammatory reaction is a hallmark of chronic and acute pathologies in the central nervous system (CNS) and greatly exacerbates neuronal degeneration. The proinflammatory cytokine tumor necrosis factor alpha (TNFα) plays a pivotal role in the initiation and progression of inflammatory processes provoking oxidative stress, eicosanoid biosynthesis, and the production of bioactive lipids. We established in neuronal cells that TNFα exposure dramatically increased Mg^{2+}-dependent neutral sphingomyelinase (nSMase) activity thus generating the bioactive lipid mediator ceramide essential for subsequent NADPH oxidase (NOX) activation and oxidative stress. Since many of the pleiotropic effects of ceramide are attributable to its metabolites, we examined whether ceramide kinase (CerK), converting ceramide to ceramide-1-phosphate, is implicated both in NOX activation and enhanced eicosanoid production in neuronal cells. In the present study, we demonstrated that TNFα exposure of human SH-SY5Y neuroblastoma caused a profound increase in CerK activity. Depleting CerK activity using either siRNA or pharmacology completely negated NOX activation and eicosanoid biosynthesis yet, more importantly, rescued neuronal viability in the presence of TNFα. These findings provided evidence for a critical function of ceramide-1-phospate and thus CerK activity in directly linking sphingolipid metabolism to oxidative stress. This vital role of CerK in CNS inflammation could provide a novel therapeutic approach to intervene with the adverse consequences of a progressive CNS inflammation.

Keywords

inflammation; ceramide kinase; NADPH oxidase; eicosanoid; oxidative stress; neuron

Corresponding Author: Thomas B. Kuhn, Department of Chemistry and Biochemistry, University of Alaska Fairbanks, 900 Yukon Drive, Fairbanks, AK 99775, (907) 474-5752 (P), (907) 474-7828 (F), tbkuhn@alaska.edu.
[c]Present Address: North Carolina Research Campus, 600 Laureate Way, Kannapolis, NC 28081

Conflict of interest statement

The Penn State Research Foundation has licensed ceramide-containing and ceramide-regulating nanoliposomes and other nanotechnologies to Keystone Nano, Inc. (State College, PA) for commercialization. MK serves as CMO of Keystone Nano, Inc.

1. Introduction

Many pathologies of the central nervous system (CNS) exhibit a strong inflammatory component that substantially contributes to neurodegeneration [1, 2]. Microglia and astrocytes respond to acute injury, toxins, or invading pathogens by secreting inflammatory mediators such as eicosanoids, cytokines, and reactive oxygen species (ROS) [3, 4]. Tumor necrosis factor alpha (TNFα), a pro-inflammatory cytokine, binds to two receptors, one coupled to the Mg^{2+}-dependent neutral sphingomyelinase (Mg^{2+}-nSMase) through the adaptor protein FAN, factor associated with nSMase [5, 6]. SMases hydrolyze sphingomyelin to produce the bioactive lipid ceramide, which is implicated in mediating oxidative stress, and other apoptotic processes [7, 8].

Ceramide, and its metabolites serve as key mediators of inflammatory pathways [9–11]. For instance, cytosolic phospholipase A_2 ($cPLA_2$), which liberates arachidonic acid (AA), translocates to distinct lipid microdomains in the endoplasmic reticulum, the Golgi apparatus, or the plasma membrane depending on the extrinsic stimulus [12, 13]. Ceramide kinase (CerK), the enzyme responsible for the phosphorylation of ceramide, is localized both in the plasma membrane and the Golgi apparatus thus establishing a connection between the production of ceramide-1-phosphate (C1P) and $cPLA_2$ activation [14–16]. More recently, it was shown that $cPLA_2$ interacts with and is activated by C1P [17]. AA is the principal product of $cPLA_2$ activity and a pivotal precursor for they biosynthesis of eicosanoids [18]. Through conversion of AA, cyclooxygenase (COX) and lipoxygenase (LOX) generate prostaglandins and leukotrienes, pleiotropic inflammatory mediators, and also significant amounts of reactive oxygen species (ROS) as byproducts [19, 20]. Moreover, AA is a critical component of membrane microdomains serving both as a membrane anchor for NADPH oxidase (NOX) as well as a cofactor for the NOX-proton channel [21–23]. In contrast to other oxidoreductases, ROS are the purposeful reaction products of NOX activity.

Utilizing a combination of pharmacological and molecular approaches, we demonstrated in human SH-SY5Y neuroblastoma cells exposed to TNFα that CerK activity was strictly required for the subsequent activation of several oxidoreductases (NOX, COX, and 5-LOX), and also enhanced eicosanoid biosynthesis as well as $cPLA_2$ activation. In addition, eliminating CerK activity rescued neuronal viability in the persistent presence of TNFα. This study demonstrated for the first time that CerK activation and thus C1P play an essential role in linking sphingolipid metabolism to increased oxidative stress thus attributing a therapeutic potential to CerK manipulation in CNS inflammation [24, 25].

2. Materials and methods

2.1. Reagents

Recombinant human tumor necrosis factor alpha (TNFα) was purchased from Millipore (Temecula, CA). DMEM and Penicillin/Streptomycin solution were obtained from Mediatech (Herndon, VA). Fetal bovine serum was received from Atlanta Biologicals (Atlanta, GA). GlutaMAX-1 and trypsin/EDTA, as well as fluorescent siRNA, were from Invitrogen (Carlsbad, CA). The Mg^{2+}-nSMase inhibitor GW4869, the aSMase inhibitor desipramine, and the CerK inhibitor K1 were from EMD Biosciences (San Diego, CA). The XTT cell proliferation kit was from Trevigen (Gaithersburg, MD). ^{3}H-arachidonic acid was from American Radiolabeled Chemicals (St. Louis, MO). All other lipids were from Avanti Polar Lipids (Alabaster, AL). The siRNA directed against CerK, and non-targeting siRNA was from Dharmacon (Lafayette, CO). A polyclonal rabbit anti-human CerK antibody was from Exalpha (Shirley, MA). A polyclonal goat anti-human phospho-$cPLA_2$ antibody, a polyclonal goat anti-human phospho-$p40^{phox}$ antibody, a polyclonal rabbit anti-human

GAPDH antibody, a polyclonal rabbit anti-human $p67^{phox}$ antibody, a monoclonal mouse anti-human β-actin antibody, and corresponding horseradish peroxidase-conjugated secondary antibodies were from Santa Cruz (Santa Cruz, CA). A polyclonal rabbit anti-human phospho-5-LOX antibody and all other reagents were purchased from Sigma (St. Louis, MO). VECTASHIELD hard set mounting medium with 4,6-diamidino-2-phenylindole (DAPI) was purchased from Vector Laboratories (Burlingame, CA). Streptavidin-agarose beads, sulfo-NHS-biotin, protease inhibitor cocktail (PIC), a Pico Super Signal chemoluminescent kit, and a BCA protein assay kit were obtained from Pierce (Rockland, IL).

2.2. Cell culture

Human SH-SY5Y neuroblastoma cells were grown in DMEM, 10% fetal bovine serum (FBS), 1% Glutamax, 100 U/ml Penicillin and 100 U/ml Streptomycin (humidified atmosphere, 5% CO_2, 37°C, 100 mm dishes Falcon). For cell harvesting, cultures were incubated with trypsin (0.5 mg/ml)/EDTA (0.2mg/ml) for 5 min, cells washed off with PBS, centrifuged (200 × g_{max}, 2 min), and resuspended in growth medium.

2.3. Cationic nanoliposome formation and siRNA loading

Aliquots of 1,2-dioleoyl-2-trimethylammonium-propane (DOTAP), 1,2-distearoyl-*sn*-glycero-3-phosphoethanolamine-N-[methoxy(polyethylene glycol)-2000] (PEG2000-DSPE), and 1,2-dioleoyl-*sn*-glycero-3-phosphoethanolamine (DOPE), suspended in chloroform, were made in a 4.75:0.5:4.75 molar ratio, or alternatively, aliquots of DOTAP, PEG2000-DSPE, DOPE, and lissamine rhodamine B-labeled DOPE were made in a 4.75:0.5:4.7025:0.0475 molar ratio. Lipids were dried to a film under a stream of nitrogen, then hydrated by addition of 0.9% NaCl to a final lipid concentration of 25 mg/ml. Solutions were sealed, heated at 60°C (60 min), mixed (Vortex), and sonicated until light no longer diffracted through the suspension. The lipid vesicle-containing solution was quickly extruded at 60°C by passing the solution 10 times through 100 nm polycarbonate filters in an Avanti Mini-Extruder (Avanti Polar Lipids, Alabaster, AL). Nanoliposome solutions were stored at 4°C until use, protected from light when necessary. To prepare siRNA-loaded cationic nanoliposomes, siRNA dissolved in 0.9% NaCl and nanoliposomes were mixed (10:1 w/w liposome to siRNA) and incubated overnight at room temperature prior to use. The RNA interference sequence was previously published by the Chalfant group (UGCCUGCUCUGUGCCUGUAdTdT and UACAGGCACAGAGCAGGCAdTdT) [17].

2.4. Confocal microscopy

Two-day old SH-SY5Y cultures (6-well plates, 5×10^5 cells per well) maintained in regular growth media were transfected with 200 nM FITC-labeled, non-targeted, siRNA loaded into rhodamine-labeled cationic nanoliposomes. After 24 h, SH-SY5Y cells were detached (0.5 mg/ml trypsin/0.2mg/ml EDTA), and replated onto glass cover slips coated with poly-D-lysine (50 μg per cm^2) in growth medium for 24 h. After three washes with PBS, cultures were fixed 2% paraformaldehyde in PBS pH 7.0 (15 min RT). Cover slips were mounted onto glass slides with DAPI-containing mounting medium. Images were acquired using a Leica scanning confocal microscope (TCS SP2 AOBS) (Bannockburn, IL), and filter combinations for FITC, rhodamine, and DAPI.

2.5. Ceramide kinase assay

SH-SY5Y cells were grown in 6-well plates (5×10^5 cells per well) for 48 h. Following transfection with either CerK-targeted siRNA, or non-targeting siRNA (200 nM, 48 h), cultures were incubated with TNFα (100 ng/ml, 15 min), washed, scraped into PBS, and sonicated. A fluorescent CerK assay, adapted for a microplate reader, was performed using

the method described by Don and Rosen [33]. Briefly, cell lysates (25 μg) were mixed with reaction buffer (100 μl, 20 mM Hepes (pH 7.4), 10 mM KCl, 15 mM $MgCl_2$, 15 mM $CaCl_2$, 10% glycerol, 1 mM DTT, 1 mM ATP) containing 10 μM NBD-labeled (green fluorescent probe) C6-ceramide conjugated to 0.2 mg/ml fatty acid-free BSA. Reactions were allowed to proceed for 30 minutes in the dark before the addition of 250 μl chloroform/methanol (2:1). Samples were vortex, centrifuged (20,000 × g_{max}, 45 s), and 100 μl of the upper aqueous phase was transferred to a 96-well (black) microplate. Dimethylformamide (100 μl) was added to each sample well and NBD fluorescence was quantified with a fluorescent microplate reader with a 495 nm excitation filter and a 525 nm emission filter.

2.6. Arachidonic acid release assay

Two-day old SH-SY5Y cultures (6-well plates, 5×10^5 cells per well) were incubated over night with 5 nM ^{3}H-arachidonic acid (0.5 μCi/ml). Next, SH-SY5Y cells were rinsed (PBS) and unincorporated radioactivity removed (1 mg/ml BSA, 10 min). After a rinse with PBS, cultures were replenished with regular growth medium and incubated either with 10 μM GW4869 (1 h), 10 μM CerK inhibitor K1 (1 h), or 200 nM siRNA (2 d). Incubations and transfection spanned the ^{3}H-arachidonic acid labeling time. Next, SH-SY5Y cells were stimulated with TNFα (100 ng/ml) and media aliquots were removed at various time points. Aliquots were centrifuged (10,000 × g_{max}, 10 min) and ^{3}H was measured in a scintillation counter (200 μl of media supernatant) to determine the relative amount of arachidonic acid metabolites released from the cells. Counts were adjusted based on the total cellular protein determined for each experimental condition (BCA protein assay).

2.7. Quantification of reactive oxygen species

SH-SY5Y cells were plated in 96-well tissue culture dishes (5×10^3 cells per well) and grown for 48 hours. Cultures were incubated (1 h) with 50 μM of the oxidation-sensitive fluorescent indicator 2′, 7′-dihydrodichlorofluorescein diacetate (H_2DCFDA) in the presence or absence of pharmacological inhibitors. H_2DCFDA is de-acetylated in the cytosol to dihydrodichlorofluorescein and increases in fluorescence upon oxidation to dichlorofluorescein (DCF) by H_2O_2. Following exposure to stimuli, cells were washed into PBS, lysed (2M Tris-Cl pH 8.0, 2% w/v SDS, 1 mM Na_3VO_4), and total DCF fluorescence intensity was quantified in 100 μl of sample cell lysates using a Beckman Coulter Multimode DTX 880 microplate reader (Fullerton, CA) with a 495 nm excitation filter and a 525 emission filter.

2.8. Cell-free NADPH oxidase assay

To measure NOX activation directly by ceramide or C1P, a cell-free method reported by Cross et al. was utilized [26, 27]. As a source of NOX components, semi-confluent SH-SY5Y cells were harvested into PBS and sonicated to completely disrupt cellular membranes into small vesicles. Crude vesicular lysates (10 μg total protein) were added to a 96-well microplate (150 μl final volume) containing reaction buffer consisting of 100 nM FAD, 100 μM cytochrome c, and either 5 μM nanoliposomal C8-ceramide or C8-C1P prepared as previously described [28]. Superoxide dismutase dissolved in PBS (300 units), or an equivalent volume of PBS, were added separately to paired sample wells. All samples were allowed to incubate at room temperature for 5 minutes. Reactions were commenced by the addition of 166 μM NADPH and the reduction of cytochrome c was quantified by measuring absorbance at 562 nm with a microplate reader. NOX activity was quantified as the superoxide dismutase-inhibitable reduction of cytochrome c (loss of absorbance).

2.9. Cellular viability assay

SH-SY5Y cells were seeded in 96-well tissue culture dishes (5×10^3 cells per well), and grown for 48 hours. Cultures were transfected with siRNA 48 h prior to other treatments. Following TNFα exposure (100 ng/ml, 48 h), XTT reagent prepared according to the manufacturer (Trevigen, Gaithersburg, MD) was added and allowed to incubate for 4 hours. Viability was determined by dual absorbance measurement (490 nm and 650 nm, our reference) using a Beckman Coulter Multimode DTX 880 microplate reader (Fullerton, CA).

2.10. Membrane translocation of $p67^{phox}$

Plasma membrane proteins were prepared by biotinylation and streptavidin-affinity chromatography as described by Li and Shah with minor modifications [29]. SH-SY5Y cells were grown in 6-well plates (5×10^5 cells per well) for 48 h. Following transfection with either CerK-targeted siRNA, or non-targeting siRNA (200 nM, 48 h), cultures were treated with TNFα (100 ng/ml, 15 min). After washing with HBSS-CM (1X HBSS, 0.1 g/l $CaCl_2$, 0.1 g/l $MgCl_2$, pH 7.5), cultures were incubated with 0.5 mg/ml sulfo-NHS-biotin (prepared in 20 mM HEPES, HBSS-CM, pH 8.0) for 40 min on ice, and excess sulfo-NHS-biotin was neutralized with 50 mM glycine (prepared in HBSS-CM) on ice for 15 min. Cells were scraped into HBSS-CM, centrifuged (200 × g_{max}, 2 min), re-suspended in 500 μL loading buffer (20 mM HEPES pH 7.5, HBSS, 1% Triton X-100, 0.2 mg/ml saponin, 1% PIC), and sonicated. Streptavidin-agarose beads (25 μL) were added to the cell lysates (2 h, 4°C). Beads were collected (2,500 × g_{max}, 2 min), re-suspended in 150 μL of loading buffer, and heated (5 min, boiling water bath). Supernatants were obtained by centrifugation (2,500 × g_{max}, 2 min), and total cellular protein content was determined (BCA protein assay). Western blotting was used to separate membrane fractions (biotinylated fraction) and antibody-labeled-$p67^{phox}$ immunoreactivity was detected by using chemoluminescence and quantified using a GE Healthcare Typhoon Imager (Piscataway, NJ) running ImageQuant software.

2.11. SDS gel electrophoresis and Western blotting

Two-day old SH-SY5Y cultures (6-well plates, 5×10^5 cells per well) were incubated with 10 μM GW4869 or 10 μM CerK inhibitor K1 prior to stimulation with 100 ng/ml TNFα (15 min). Cells were lysed (2 M Tris-Cl pH 8.0, 2% SDS, 1 mM Na_3VO_4) and supernatants collected following centrifugation (3,000 × g_{max}, 4°C, 20 min). Equal amounts of total protein (5–50 μg, BCA protein assay) were separated by SDS-polyacrylamide (10–15%) gel electrophoresis (125 volts, 50 watts, 75 mA) and proteins transferred onto nitrocellulose or PVDF membranes (2.5 hours, 50 volts, 50 watts, 250 mA) according to Towbin and coworkers [30, 31]. Following transfer, membranes were blocked with TBST-BSA (5 mg/ml BSA, 50 mM Tris-Cl pH 7.4, 150 mM NaCl, 0.1% Tween-20), and probed overnight with the appropriate primary antibody (1 μg/μl in TBST). Following incubation with a corresponding horseradish peroxidase-conjugated secondary antibody (0.2 μg/μl in TBST, 45 min), immunoreactivity was detected by film exposure, followed by NIH ImajeJ analysis (Bethesda, MD).

2.12. Statistical analysis

One-way and or two-way ANOVA, or t-tests were used to determine statistically significant differences between treatments ($p<0.05$). At least three independent experiments were performed for each condition with a minimum of duplicate cell cultures. *Post hoc* comparisons of specific treatments were performed using a Bonferroni multiple comparisons test. All error bars represent standard error from the mean (SEM). All statistical analyses were carried out using GraphPad Prism 4 software (La Jolla, CA).

3. Results

3.1. TNFα stimulates multiple ROS generating sources in SH-SY5Y neuroblastoma cells

Oxidative stress is a hallmark of acute, chronic, and certain psychiatric pathologies of the CNS and accompanies inflammatory processes [1, 2]. Numerous studies have demonstrated that TNFα causes oxidative stress in many non-neuronal and neuronal cell types both *in vivo* and *in vitro* [3, 32]. We assessed in human SH-SY5Y neuroblastoma cells whether TNFα-mediated oxidative stress was attributable to the three oxidoreductases NOX, COX, or 5-LOX all implicated in inflammatory responses. To quantify intracellular ROS production, SH-SY5Y cells were loaded with the oxidation-sensitive fluorescent indicator 2′, 7′-dihydrodichlorofluorescein (DCF). Acute exposure of SH-SY5Y cells to 100 ng/ml TNFα (15 min) significantly increased DCF-fluorescence intensity (1.43 ± 0.03, n=4) compared to control (1.00 ± 0.03, n=4) indicative of a generation of intracellular ROS (Fig. 1). TNFα-stimulated ROS formation was blocked upon preincubation (1 h) of SH-SY5Y cells with the NOX inhibitor diphenylene iodonium (10 μM DPI, 1.02 ± 0.03, n=4), the COX inhibitor indomethacin (10 μM IDM, 0.87 ± 0.02, n=4), the 5-LOX activator-protein inhibitor MK-886 (10 μM MK, 1.02 ± 0.05, n=4), or the antioxidant N-acetyl-L-cysteine (5 mM NAC, 0.34 ± 0.003, n=4). It is noteworthy that treatment with the antioxidant NAC even in the absence of TNFα dramatically lowered ROS indicative of a substantial endogenous redox state. Thus, NOX, COX, and 5-LOX were all implicated as sources of ROS formation in SH-SY5Y cells exposed to TNFα.

Ceramide generation is well documented in response to various stimuli including pro-inflammatory cytokines [11]. Previously, we had demonstrated that TNFα exposure of SH-SY5Y cells or primary cortical neurons stimulated a Mg^{2+}-dependent neutral sphingomyelinase (nSMase) activity critical for the stimulation of NOX and subsequent oxidative stress [33]. In this study, TNFα-stimulated intracellular ROS production was blocked in SH-SY5Y cells when preventing sphingomyelin hydrolysis to ceramide with the Mg^{2+}-nSMase inhibitor GW4869 (10 μM GW, 1.09 ± 0.02, n=4), as well as the acid sphingomyelinase (aSMase) inhibitor desipramine (10 μM DES, 1.11 ± 0.05, n=4). Likewise, TNFα-stimulated intracellular ROS production was negated with K1, ceramide kinase inhibitor (10 μM, 0.95 ± 0.07, n=4). Taken together, these findings indicated that both generation of ceramide via Mg^{2+}-nSMase or aSMase activity as well as conversion of ceramide to C1P by CerK activity were necessary in ROS production in SH-SY5Y cells upon exposure to TNFα.

3.2. TNFα stimulates CerK activity in SH-SY5Y neuroblastoma cells

To further investigate the role of CerK, we used a well-characterized siRNA sequence against CerK previously validated by the Chalfant lab to specifically knockdown CerK expression in SH-SY5Y cells [34]. We utilized a novel cationic nanoliposome formulation to transfect SH-SY5Y cells with siRNA, a formulation specifically designed for *in vivo* systemic delivery and virtually non-toxic [35]. Two days post-delivery, we validated liposomal delivery of siRNA into SH-SY5Y cells through fluorescence tags on either the siRNA or on the liposome itself. Whereas siRNA was present in perinuclear and cytoplasmic regions of the cells (green fluorescence), liposome components incorporated into the plasma membranes of cells (red fluorescence) (Fig, 2A). Furthermore, nanoliposomal delivery of siRNA (200 nM) resulted in a 73% efficiency of transfection two days post-delivery. Western blotting demonstrated a significant knockdown of CerK with 200 nM CerK-targeted siRNA (siCK, 25% ± 9%, n=3) compared to non-targeted siRNA (siSCR, 100% ± 13%, n=3) (Fig. 2B). Most importantly, transfection of SH-SY5Y neuroblastoma cells with 200 nM CerK-targeted siRNA completely blocked TNFα-stimulated CerK activity (TNF+siCK, 0.96 ± 0.11, n=3) whereas 200 nM non-targeted

siRNA was ineffective (TNF+siSCR, 2.62 ± 0.55, n=3) (Fig. 2C). Together these results demonstrated that CerK-targeted siRNA delivered by cationic nanoliposome was highly effective in depleting CerK activity and in negating Cerk activation in SH-SY5Y cells in response to TNFα.

3.3. Blocking CerK abolishes neuronal NOX activity in response to TNFα

Previously, we demonstrated that TNFα stimulated Mg^{2+}-nSMase activity preceding intracellular ROS production by NOX in SH-SY5Y cells [33]. Since C1P is implicated in inflammatory processes and AA production by $cPLA_2$, a lipid activator of NOX, we examined whether CerK activation and thus production of C1P is critical for TNFα-mediated NOX activation in SH-SY5Y cells. As shown in Figure 3, 100 ng/ml TNFα (15 min) stimulated a robust intracellular ROS production (TNF, 1.94 ± 0.19, n=4) compared to control (CON, 1.00 ± 0.13, n=4) (Fig. 3A). Notably, depleting CerK activity with targeted siRNA (200 nM, 48 h) completely abolished TNFα-stimulate ROS production (TNF+siCK, 1.05 ± 0.1, n=4) as opposed to non-targeted siRNA (TNF+siSCR, 1.68 ± 0.08, n=4). Most importantly, depletion of CerK in SH-SY5Y cells prior to TNFα exposure disrupted the functional assembly of NOX, multi-subunit protein complex comprised of both cytosolic and plasma membrane subunits, essential for ROS production (Fig. 3B). Exposure of SH-SY5Y cells to TNFα (15 min, 100 ng/ml) caused a significant association of the cytosolic NOX subunit $p67^{phox}$ with plasma membrane (2.26 ± 0.16, n=3) compared to control (1.00 ± 0.04, n=3). CerK depletion utilizing CerK-targeted siRNA (200 nM, 48 h) completely negated association of $p67^{phox}$ with plasma membranes (TNF+siCK, 1.23 ± 0.19, n=3) despite a presence of TNFα as opposed to non-targeted siRNA (TNF+siSCR, 2.12 ± 0.19, n=3). To evaluate directly a role for C1P in mediating NOX activation, we employed a cell free system containing plasma membrane vesicles as adapted from Cross et al. [34–36] (Fig. 3C). Although NOX activity was stimulate by the addition of nanoliposomal ceramide, supplementing the cell free system with nanoliposomal C1P increased NOX activity almost 3 fold. Together, these results demonstrated that CerK activity and its product, the ceramide metabolite C1P, were essential in mediating NOX activation in SH-SY5Y cells upon exposure to TNFα.

We further assessed whether depleting CerK activity in SH-SY5Y cells would proof beneficial to the viability of neuronal cells in the persistent presence of TNFα since CerK activity was required for NOX-dependent oxidative stress (Fig. 3D). Persistent presence of 100 ng/ml TNFα over 48 h significantly decreased viability of SH-SY5Y cells (67% ± 2%, n=12) compared to control (100% ± 4%, n=12). Indeed, depleting CerK activity with targeted siRNA (200 nM, 48 h) protected SH-SY5Y viability in the presence of TNFα (85% ± 3%, n=8) whereas non-targeted siRNA was ineffective (68% ± 2%, n=8). Importantly, viability results were normalized to account for minor toxicity observed with CerK-targeted siRNA treatment alone hence demonstrating a vital role for CerK in basal SH-SY5Y physiology. However, overstimulation of CerK activity by TNFα greatly compromises neuronal viability. These findings provided strong evidence that CerK activity is central to mediating oxidative stress and contributing to neuronal degeneration in the persistent presence of an inflammatory stimulus.

3.4. Eliminating CerK activity impedes release of arachidonic acid metabolites from SH-SY5Y cells exposed to TNFα

Phosphorylation of many proteins regulates both activity status and/or subcellular localization. Relevant to our studies, phosphorylation of $cPLA_2$ results in conformational changes exposing lipid-binding domains essential for its proper function [36]. With regard to NOX, phosphorylation of the cytosolic NOX subunits $p47^{phox}$ and $p40^{phox}$ key enables both interactions with target membranes and the membrane-bound NOX subunits [37–39].

Phosphorylation of 5-LOX at Ser^{523} is thought to regulate its localization [40]. In SH-SY5Y cells, phosphorylation of $cPLA_2$ increased following a 15 min addition of 100 ng/ml TNFα compared to control, yet was blocked in the presence (1 h) of the Mg^{2+}-nSMase inhibitor GW4869 (10 μM) or the CerK inhibitor K1 (10 μM) (Fig. 4A). Likewise, pharmacological inhibition of Mg^{2+}-nSMase or CerK blocked similar TNFα triggered phosphorylation of the $p40^{phox}$ NOX subunit and phosphorylation of 5-LOX (Fig. 4A). These data confirmed that the proinflammatory cytokine TNFα signaled the activation of $cPLA_2$ and 5-LOX in neuronal cells generating key precursors for eicosanoid biosynthesis aside from stimulating NOX.

The oxidoreductases COX and LOX are responsible for the oxygenation of AA, the initial step in eicosanoid biosynthesis and an important element of inflammatory processes [18]. To the release of AA metabolites from SH-SY5Y cells, we incubated SH-SY5Y cells with ^3H-labeled arachidonic acid (overnight) and determined ^3H-release into the medium as a function of TNFα exposure and manipulation of CerK activity (Fig. 4B). SH-SY5Y cells exposed to 100 ng/ml of TNFα released substantially greater amounts of AA metabolites over a six hour-time course (TNFα, 6 h, 482 ± 46 cpm, n=3) compared to control (6 h, 223 ± 24 cpm, n=3). Eliminating CerK activity with CerK-targeted siRNA (200 nM, 48 h) significantly blocked the release of AA metabolites in the presence of TNFα (TNFα+siCK, 6 h, 176 ± 23 cpm, n=3) as opposed to non-targeted siRNA (TNFα+siSCR, 6 h, 525 ± 50 cpm, n=3). Moreover, pharmacological inhibition of CerK activity with 10 μM K1 (1 h) or preventing ceramide formation by inhibiting Mg^{2+}-nSMase with 10 μM GW4869 interfered with the release of AA metabolites upon exposure to TNFα (TNFα+K1, 6 h, 274 ± 25 cpm, n=3 and TNFα+GW, 6 h, 291 ± 35 cpm, n=3, respectively). These findings provided evidence that CerK activity in response to the inflammatory stimulus TNFα was essential for enhanced biosynthesis and release of eicosanoids.

4. Discussion

A progressive and persistent inflammation associated with CNS injuries and disorders exhibits a distinctive deregulation of lipid metabolism and redox homeostasis in particular a disruption of sphingolipid metabolism, increased oxidative stress, and enhanced eicosanoid biosynthesis [10, 11, 19, 32]. The proinflammatory cytokine TNFα instigates these cellular stress conditions with its capacity to elicit an accumulation of ceramide and ROS. Our findings revealed that TNFα stimulated multiple oxidoreductases in SH-SY5Y neuroblastoma cells including COX, 5-LOX, and NOX all generating substantial quantities of ROS hence increasing oxidative stress. Moreover, ROS production was sensitive to pharmacological inhibition of Mg^{2+}-nSMase, aSMase, and ceramide kinase indicating that ceramide and its metabolite C1P were essential in linking disruption of sphingolipid metabolism to oxidative stress (Fig. 5). Our studies established for the first time a novel role for CerK and its product C1P in intracellular signaling and inflammation as a prerequisite for NOX-dependent ROS formation and eicosanoid biosynthesis in neuronal cells [16, 24, 41].

In essence, two principal scenarios could explain the C1P-dependent regulation of NOX activity revealed in our study. As an indirect regulator, C1P could influence NOX activity through its effects on $cPLA_2$ and subsequent AA production. C1P directly binds $cPLA_2$ enabling membrane association of $cPLA_2$ and hence greatly stimulating $cPLA_2$ activity [17]. The resulting increases in AA would further facilitate membrane targeting of NOX subunits as well as activating the proton channel of the $gp91^{phox}$ membrane-bound subunit [22, 23, 42]. Moreover, AA is the principal substrate for both LOX and COX and AA production is the rate-limiting step of eicosanoid biosynthesis [19]. It is noteworthy that the AA

metabolites 15-deoxy-Delta (12, 14)-prostaglandin J_2 and leukotriene B_4 were shown to stimulate NOX activity [20].

However, more direct roles for C1P as a regulator of NOX activity are plausible alternatives particularly with respect to the time course of NOX activation. Utilizing a cell free system containing plasma membrane vesicles, supplementation with C1P significantly stimulated NOX activity within minutes (Fig. 3) comparable to the time frame of CerK stimulation and NOX activation in intact SH-SY5Y cells exposed to TNFα (15 min). In contrast, a significant production of AA and metabolites in response to TNFα was considerably slower (1 h or more) (Fig. 4). Together, these findings suggest that TNFα-mediated formation of C1P precedes that of AA. Possibly, C1P could serve as a membrane anchor for NOX subunits in analogy its role for $cPLA_2$ although this remains to be demonstrated. ROS production by NOX or LOX requires phosphorylation of protein subunits inducing conformational changes essential for subcellular distribution and activation [37, 38]. Protein kinase C isoforms, protein kinase A, and Erk kinases are not only responsible for the phosphorylation of LOX and NOX subunits but also exhibit C1P-dependent regulation [43, 44]. Lastly, functional assembly of cytosolic and plasma membrane subunits of NOX preferentially occurs in lipid rafts, heterogeneous plasma membrane regions characterized by unique a lipid and protein repertoire, membrane curvature, and tethering to the actin cytoskeleton [45–47]. Signaling capacities of lipid rafts are differentially shaped by distinct lipid species discretely altering membrane fluidity, thickness, and/or curvature all affecting protein-protein interactions, lipid protein interactions, protein conformation, and enzymatic activities [48, 49]. Ceramide and its metabolites harbor a vital role in the formation and reorganization of lipid rafts altering membrane fluidity and thickness [50–52]. Increases in ceramide supports lipid raft formation and coalescence of raft domains [50, 52, 53]. The role of C1P in lipid raft formation is more controversial yet increased levels of membrane C1P supported fluidity over rigidity [54]. However, increases in CerK activity and presumably increases in C1P supported lipid raft formation in phagocytic cells [55]. Thus, our results favor a direct regulatory role of C1P in NOX activation and ROS production. TNFα stimulates the coalescence of large lipid raft macrodomains in SH-SY5Y neuroblastoma cells (data not shown) [56]. It is noteworthy that a loss of CerK activity substantially rescued the viability of SH-SY5Y neuroblastoma cells in the presence of TNFα. Depletion of CerK activity via targeted siRNA utilized a novel cationic nanoliposome, which is highly suited and designed specifically for *in vivo* applications due to its minimal cytotoxicity [35].

In summary, this study established for the first time an essential role of CerK in regulating NOX activation and subsequent ROS formation as well as COX/LOX-mediated eicosanoid biosynthesis in neuronal cells. Consequently, manipulation of CerK activity and hence the metabolite C1P could potentially open new therapeutic strategies to alleviate neuronal stress and improve neuronal survival in CNS inflammation.

Acknowledgments

This study was supported by National Institutes of Health U54 grant NS41069 (SNRP: NINDS, NIMH, NCRR, NCMHD), and United States Department of Agriculture grant 2005-34495-16519 (TBK).

Abbreviations

aSMase	acid sphingomyelinase
AA	arachidonic acid
BSA	bovine serum albumin

C1P	ceramide-1-phosphate
CerK	ceramide kinase
COX	cyclooxygenase
cPLA$_2$	cytosolic phospholipase A$_2$
DAPI	4,6-diamidino-2-phynelindole
DCF	dichlorofluorescein
DOPE	1,2-dioleoyl-*sn*-glycero-3-phosphoethanolamine
DOTAP	1,2-dioleoyl-2-trimehtylammonium-propane
DPI	diphenylene iodonium
FBS	fetal bovine serum
FITC	fluorescein
H$_2$DCFDA	2′,7′-dihydrodichlorofluorescein diacetate
HBSS-CM	Hank's balanced salt solution with Ca^{2+} and Mg^{2+}
IDM	indomethacin
LOX	lipooxygenase
Mg2+-nSMase	Mg^{2+}-dependent neutral sphingomyelinase
MK	MK-886
NAC	N-acetyl-L-cysteine
NBD	N-4-nitrobenzo-2-oxa-1,3-diazole
NOX	NADPH oxidase
PBS	phosphate buffered saline
PIC	protease inhibitor cocktail
PEG2000-DSPE	1,2-distearoyl-*sn*-glucero-3-phosphoethanolamine-N-[methoxy(polyethylene glycol)-2000]
ROS	reactive oxygen species
SMase	sphingomyelinase
TNFα	tumor necrosis factor alpha

References

1. Amor S, Puentes F, Baker D, van der Valk P. Immunology. 2010; 129:154–169. [PubMed: 20561356]
2. Lucas SM, Rothwell NJ, Gibson RM. Br J Pharmacol. 2006; 147(Suppl 1):S232–240. [PubMed: 16402109]
3. Block ML, Zecca L, Hong JS. Nat Rev Neurosci. 2007; 8:57–69. [PubMed: 17180163]
4. Polazzi E, Contestabile A. Rev Neurosci. 2002; 13:221–242. [PubMed: 12405226]
5. Adam-Klages S, Adam D, Wiegmann K, Struve S, Kolanus W, Schneider-Mergener J, Kronke M. Cell. 1996; 86:937–947. [PubMed: 8808629]
6. Haubert D, Gharib N, Rivero F, Wiegmann K, Hosel M, Kronke M, Kashkar H. Embo J. 2007; 26:3308–3321. [PubMed: 17599063]

7. Clarke CJ, Snook CF, Tani M, Matmati N, Marchesini N, Hannun YA. Biochemistry. 2006; 45:11247–11256. [PubMed: 16981685]
8. Marchesini N, Hannun YA. Biochem Cell Biol. 2004; 82:27–44. [PubMed: 15052326]
9. Arana L, Gangoiti P, Ouro A, Trueba M, Gomez-Munoz A. Lipids Health Dis. 2010; 9:15. [PubMed: 20137073]
10. Nixon GF. Br J Pharmacol. 2009; 158:982–993. [PubMed: 19563535]
11. Milhas D, Clarke CJ, Hannun YA. FEBS Lett. 2010; 584:1887–1894. [PubMed: 19857494]
12. Evans JH, Gerber SH, Murray D, Leslie CC. Mol Biol Cell. 2004; 15:371–383. [PubMed: 13679516]
13. Jupp OJ, Vandenabeele P, MacEwan DJ. Biochem J. 2003; 374:453–461. [PubMed: 12786601]
14. Bornancin F. Cell Signal. 2011; 23:999–1008. [PubMed: 21111813]
15. Carre A, Graf C, Stora S, Mechtcheriakova D, Csonga R, Urtz N, Billich A, Baumruker T, Bornancin F. Biochem Biophys Res Commun. 2004; 324:1215–1219. [PubMed: 15504344]
16. Chalfant CE, Spiegel S. J Cell Sci. 2005; 118:4605–4612. [PubMed: 16219683]
17. Pettus BJ, Bielawska A, Subramanian P, Wijesinghe DS, Maceyka M, Leslie CC, Evans JH, Freiberg J, Roddy P, Hannun YA, Chalfant CE. J Biol Chem. 2004; 279:11320–11326. [PubMed: 14676210]
18. Brock TG, Peters-Golden M. Scientific World Journal. 2007; 7:1273–1284. [PubMed: 17767350]
19. Khanapure SP, Garvey DS, Janero DR, Letts LG. Curr Top Med Chem. 2007; 7:311–340. [PubMed: 17305573]
20. Cho KJ, Seo JM, Kim JH. Mol Cells. 2011; 32:1–5. [PubMed: 21424583]
21. Groemping Y, Rittinger K. Biochem J. 2005; 386:401–416. [PubMed: 15588255]
22. Henderson LM, Thomas S, Banting G, Chappell JB. Biochem J. 1997; 325(Pt 3):701–705. [PubMed: 9271091]
23. Mankelow TJ, Pessach E, Levy R, Henderson LM. Biochem J. 2003; 374:315–319. [PubMed: 12765544]
24. Saxena S, Banerjee M, Shirumalla RK, Ray A. Curr Opin Investig Drugs. 2008; 9:455–462.
25. Lamour NF, Chalfant CE. Curr Drug Targets. 2008; 9:674–682. [PubMed: 18691014]
26. Cross AR, Erickson RW, Curnutte JT. The Journal of biological chemistry. 1999; 274:15519–15525. [PubMed: 10336445]
27. Cross AR, Erickson RW, Curnutte JT. Biochem J. 1999; 341(Pt 2):251–255. [PubMed: 10393079]
28. Barth BM, Gustafson SJ, Young MM, Shanmugavelandy SS, Kaiser JM, Cabot MC, Kester M, Kuhn TB. Cancer Biology and Therapy, DIO. 2010
29. Li JM, Shah AM. J Biol Chem. 2002
30. Laemmli UK. Nature. 1970; 227:680–685. [PubMed: 5432063]
31. Towbin H, Staehelin T, Gordon J. Proc Natl Acad Sci U S A. 1979; 76:4350–4354. [PubMed: 388439]
32. Adibhatla RM, Hatcher JF. Subcell Biochem. 2008; 49:241–268. [PubMed: 18751914]
33. Barth GSBM, Kuhn TB. J Neurosci Res. 2011 in press.
34. Lamour NF, Stahelin RV, Wijesinghe DS, Maceyka M, Wang E, Allegood JC, Merrill AH Jr, Cho W, Chalfant CE. J Lipid Res. 2007; 48:1293–1304. [PubMed: 17392267]
35. Tran MA, Gowda R, Sharma A, Park EJ, Adair J, Kester M, Smith NB, Robertson GP. Cancer Res. 2008; 68:7638–7649. [PubMed: 18794153]
36. Das S, Rafter JD, Kim KP, Gygi SP, Cho W. The Journal of biological chemistry. 2003; 278:41431–41442. [PubMed: 12885780]
37. El-Benna J, Dang PM, Gougerot-Pocidalo MA, Marie JC, Braut-Boucher F. Exp Mol Med. 2009; 41:217–225. [PubMed: 19372727]
38. Fontayne A, Dang PM, Gougerot-Pocidalo MA, El-Benna J. Biochemistry. 2002; 41:7743–7750. [PubMed: 12056906]
39. Massenet C, Chenavas S, Cohen-Addad C, Dagher MC, Brandolin G, Pebay-Peyroula E, Fieschi F. J Biol Chem. 2005; 280:13752–13761. [PubMed: 15657040]

40. Luo M, Jones SM, Flamand N, Aronoff DM, Peters-Golden M, Brock TG. The Journal of biological chemistry. 2005; 280:40609–40616. [PubMed: 16230355]
41. Gomez-Munoz A, Gangoiti P, Granado MH, Arana L, Ouro A. Adv Exp Med Biol. 2010; 688:118–130. [PubMed: 20919650]
42. Daniels I, Lindsay M, Keany C, Burden R, Fletcher J. A Haynes Clinical and Diagnostic Laboratory Immunology. 1998; 5:683–689.
43. Gangoiti P, Granado MH, Arana L, Ouro A, Gomez-Munoz A. FEBS letters. 2010; 584:517–524. [PubMed: 19948174]
44. Shimizu M, Tada E, Makiyama T, Yasufuku K, Moriyama Y, Fujino H, Nakamura H, Murayama T. Cell Signal. 2009; 21:440–447. [PubMed: 19101626]
45. Simons K, Toomre D. Nat Rev Mol Cell Biol. 2000; 1:31–39. [PubMed: 11413487]
46. Lingwood D, Simons K. Science. 2010; 327:46–50. [PubMed: 20044567]
47. Jin S, Zhou F, Katirai F, Li PL. Antioxid Redox Signal. 2011
48. Cremesti AE, Goni FM, Kolesnick R. FEBS Lett. 2002; 531:47–53. [PubMed: 12401201]
49. Harder T. Philos Trans R Soc Lond B Biol Sci. 2003; 358:863–868. [PubMed: 12803918]
50. Bollinger CR, Teichgraber V, Gulbins E. Biochim Biophys Acta. 2005; 1746:284–294. [PubMed: 16226325]
51. van Blitterswijk WJ, van der Luit AH, Veldman RJ, Verheij M, Borst J. Biochem J. 2003; 369:199–211. [PubMed: 12408751]
52. Johnston I, Johnston LJ. Langmuir. 2006; 22:11284–11289. [PubMed: 17154617]
53. Ira, Johnston LJ. Biochim Biophys Acta. 2008; 1778:185–197. [PubMed: 17988649]
54. Morrow MR, Helle A, Perry J, Vattulainen I, Wiedmer SK, Holopainen JM. Biophys J. 2009; 96:2216–2226. [PubMed: 19289048]
55. Hinkovska-Galcheva V, Boxer LA, Kindzelskii A, Hiraoka M, Abe A, Goparju S, Spiegel S, Petty HR, Shayman JA. The Journal of biological chemistry. 2005; 280:26612–26621. [PubMed: 15899891]
56. Lotocki G, Alonso OF, Dietrich WD, Keane RW. J Neurosci. 2004; 24:11010–11016. [PubMed: 15590916]

Highlights

- TNFα stimulates ceramide kinase in neuronal cells
- Ceramide-1-phosphate directly activates a neuronal NADPH oxidase activity.
- Ceramide kinase activity is necessary for TNFα-stimulated eicosanoid biosynthesis in neuronal cells.

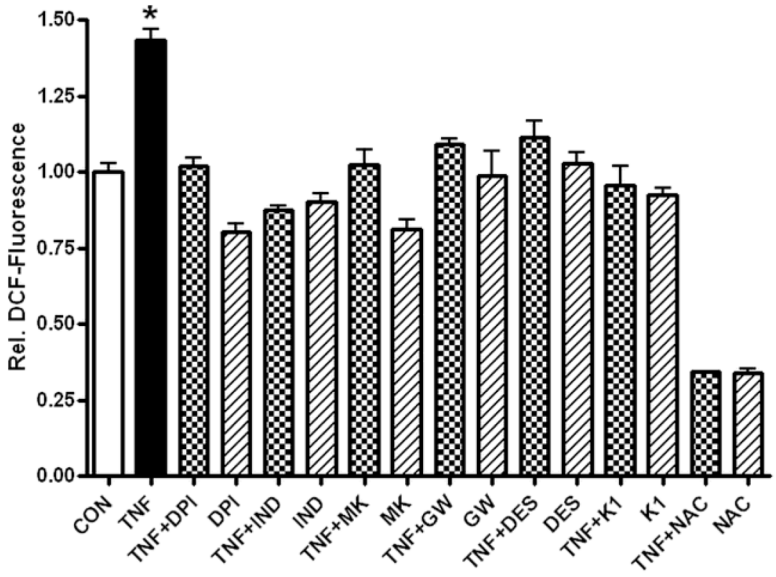

Fig. 1.

TNFα stimulates neuronal ROS production by oxidoreductas in a ceramide-dependent manner. SH-SY5Y neuroblastoma cells were exposed to TNFα (100 ng/ml, 15 min) and the production of intracellular ROS was quantified using the oxidation-sensitive fluorescent indicator 2′, 7′-dihydrodichlorofluorescein (DCF). Pre-treatment of cells for one hour with pharmacological inhibitors blocking NOX (10 μM diphenylene iodonium, DPI), COX (10 μM indomethacin, IND), the 5-LOX activator protein (10 μM MK-886, MK), Mg^{2+}-nSMase (10 μM GW4869, GW), aSMase (10 μM desipramine, DES), or CerK (10 μM K1), or 5 mM of the antioxidant N-acetyl-L-cysteine (NAC), prevented TNFα-stimulated ROS production. One-way ANOVA, *$p<0.01$ compared to all conditions, n=4.

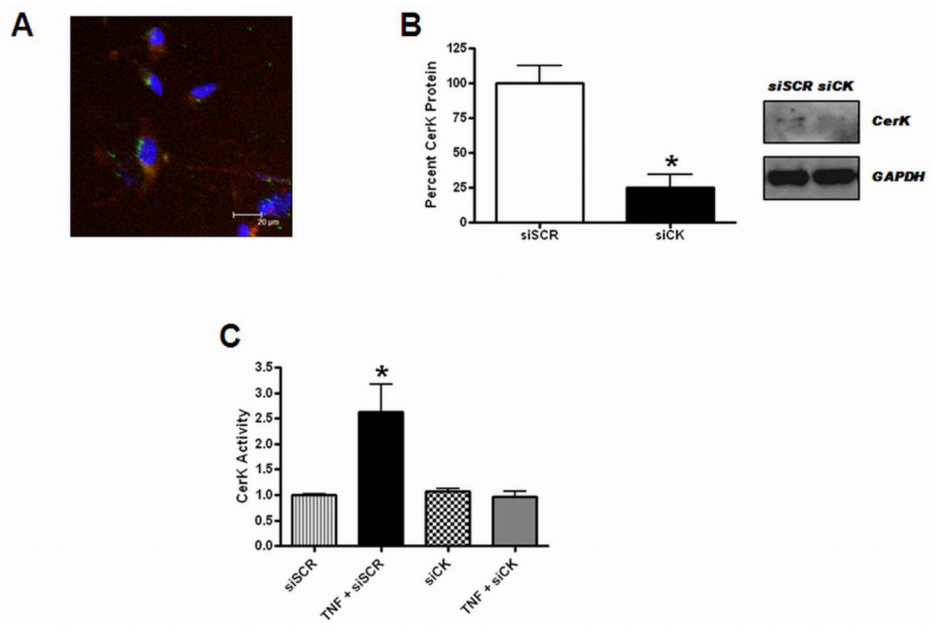

Fig. 2.

TNFα stimulates CerK activity. Cationic nanoliposomes were utilized to deliver siRNA (200nM, 48 h) to SH-SY5Y cells. (A) Fluorescent confocal microscopy revealed delivery of fluorescently labeled siRNA (green), and liposome components (red), to DAPI-labeled cells (blue). (B) Western blotting revealed effective knockdown of CerK with targeted-siRNA (siCK) compared with non-targeted siRNA (siSCR). Unpaired t-test, *$p<0.01$, n=3. (C) TNFα-stimulated CerK activity was abrogated by CerK-targeted siRNA but not non-targeted siRNA. One-way ANOVA, *$p<0.05$ compared to all conditions, n=3.

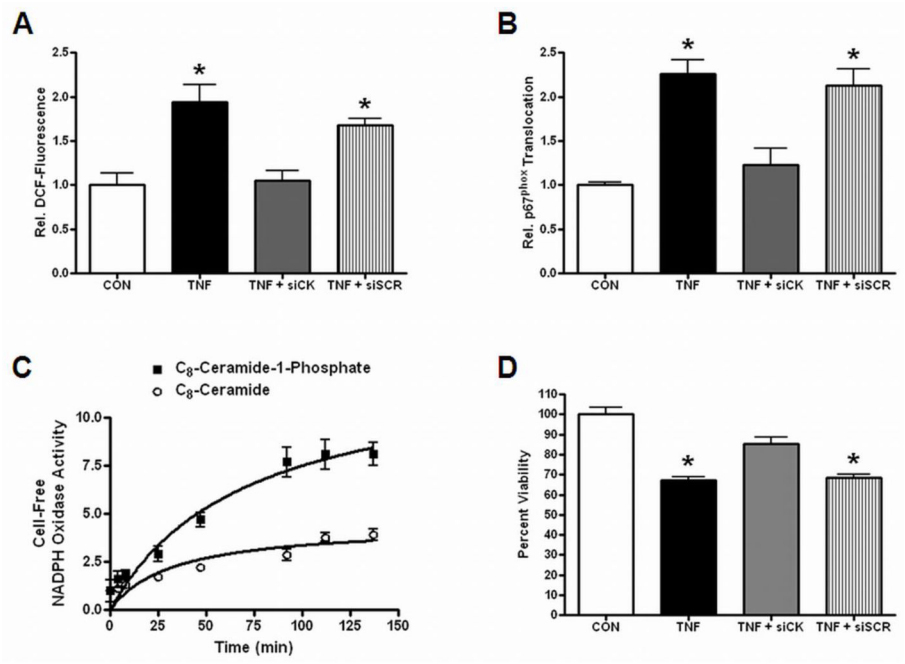

Fig. 3.

CerK activity is necessary for TNFα-stimulated NOX function in neuronal cells. Nanoliposomal-delivered siRNA (200 nM, 48 h) was used to knockdown CerK in SH-SY5Y cells prior to exposure to 100 ng/ml TNFα. (A) Intracellular ROS production was quantified using the oxidation-sensitive fluorescent indicator 2′, 7′-dihydrodichlorofluorescein (DCF). CerK-targeted siRNA (siCK), but not non-targeted siRNA (siSCR), abrogated TNFα-stimulated (15 min) ROS production. One-way ANOVA, *$p<0.05$ compared to untreated control (CON) and TNF+siCK, n=4. (B) Translocation of the cytosolic NOX subunit $p67^{phox}$ to the plasma membrane was evaluated. Nanoliposomal-delivered siCK, but not non-targeted siSCR, abrogated TNFα-stimulated (15 min) $p67^{phox}$ translocation to the plasma membrane. One-way ANOVA, *$p<0.05$ compared to CON and TNF+siCK, n=3. (C) Nanoliposomal short-chain (C8) C1P was shown to directly stimulate NOX in a cell-free assay while nanoliposomal short-chain (C8) ceramide only did so minimally. Cell-free NOX activity was measured as superoxide-inhibitable cytochrome c reduction in a solution utilizing lysed SH-SY5Y cells as a source for NOX components. A non-linear regression was used to fit curves to the observed data. Two-way ANOVA revealed that the curves were significantly different beyond 48 minutes ($p<0.001$, n=6 per time point). (D) Nanoliposomal-delivered siCK, but not non-targeted siSCR, prevented TNFα-stimulated (48 h) loss of cellular viability. One-way ANOVA, *$p<0.01$ compared to CON and TNF +siCK, n=8.

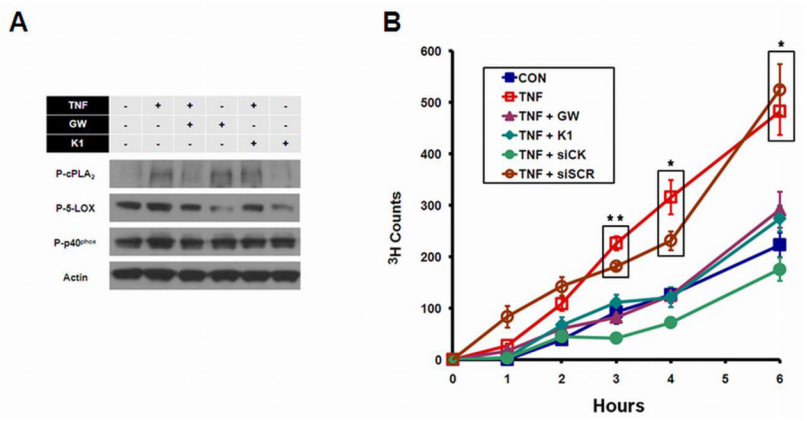

Fig. 4.

CerK regulates TNFα-stimulated eicosanoid biosynthesis in neuronal cells. (A) Eicosanoid biosynthesis and NOX activity are closely tied to the production of arachidonic acid (AA) by $cPLA_2$. Phosphorylation has been shown to be an important step in the activation of numerous enzymes. In SH-SY5Y cells, phosphorylation of $cPLA_2$, 5-LOX, and the $p40^{phox}$ cytosolic subunit of NOX, increased following exposure to TNFα (100 ng/ml, 15 min), yet was blocked by pre-treatment (1 h) with the Mg^{2+}-nSMase inhibitor GW4869 (10 μM, GW) or the CerK inhibitor K1 (10 μM). (B) SH-SY5Y cells were labeled with ^{3}H-AA overnight, treated for one hour with10 μM GW4869, 10 μM K1 or alternatively transfected with CerK-targeted or non-targeted siRNA (200 nM, 48 h), and then exposed to TNFα (100 ng/ml). Aliquots of growth medium were collected regularly over a 6 h time period and release of AA metabolites was quantified as ^{3}H-counts (scintillation counting). All data was adjusted to total cellular protein. TNFα stimulated a significant release of release of AA metabolites (TNF, open squares) compared to control (CON, closed squares). Eliminating CerK activity with targeted siRNA impeded release of AA metabolites (siCK, closed cirlces) whereas non-targeted siRNA was ineffective (siCR, open circles). Depleting ceramide, the CerK substrate, by inhibiting Mg^{2+}-nSMase (GW, filled triangles) or blocking CerK activity (K1, filled diamonds) also reduced release of AA metabolites. Boxes denote significantly different values. Two-way ANOVA, *$p<0.01$, compared to all other treatments, **$p<0.01$ compared to all treatments except TNF + K1, n=3.

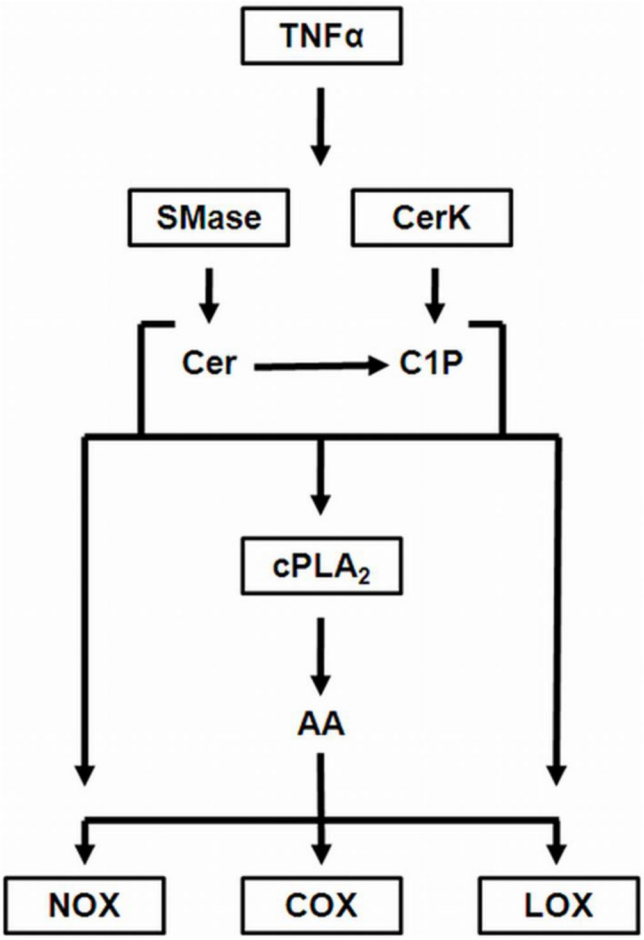

Fig. 5.

CerK harbors a central role in regulating NOX activity and eicosanoid biosynthesis in neuronal cells in response to TNFα. TNFα promotes an accumulation of ceramide metabolites through two principal activities: i) SMase activity hydrolyzing sphingymyelin to ceramide (Cer), and ii) CerK activity, which converts ceramide to C1P. Arachidonic acid (AA) generated by C1P-stimulated $cPLA_2$ serves as a substrate for eicosanoid biosynthesis via cyclooxygenase (COX) and lipoxygenase (LOX) activity. AA, ceramide, and C1P can also directly influence the activity of NOX.